Synthesis and Characterization of Novel Donor–Acceptor Naphthoquinone Derivatives with Photoinduced Charge–Transfer Properties. A Joint Experimental and Theoretical Study

Beatriz Illescas, Nazario Martín,* José L. Segura, and Carlos Seoane*

Departamento de Química Orgánica, Facultad de Química, Universidad Complutense, E-28040 Madrid, Spain

Enrique Ortí, Pedro M. Viruela, and Rafael Viruela

Departamento de Química Física, Universidad de Valencia, E-46100 Burjassot (Valencia), Spain

Received February 24, 1995[⊗]

The synthesis of substituted benzo[*b*]phenoxazine-6,11-diones (**7a–d**) and their precursor *N*-tosyl derivatives (**6a–d**) is reported. The *N*-methylbenzo[*b*]phenoxazine-6,11-dione (**8**) and the analogous benzo[*b*]phenothiazine-6,11-dione (**9**) are also prepared. The UV-vis spectra of compounds **6**, **7**, and **9** show the existence of an intramolecular electronic transfer from the respective benzoxazine or benzothiazine donor fragments to the acceptor *p*-benzoquinone moiety. In agreement with this donor–acceptor character, the cyclic voltammograms of **7–9** exhibit two one-electron reduction waves to the corresponding radical-anion and dianion and two quasireversible oxidation peaks; however, the tosyl group in compounds **6** results in only one quasireversible oxidation wave at higher positive values. This causes a strong hypsochromic shift of the low-energy charge-transfer band. The molecular and electronic structures of compounds **6-8** are investigated using the semiempirical PM3 method and the nonempirical VEH approach, respectively. PM3 calculations predict that both the neutral and the reduced/oxidized compounds are nonplanar, the largest distortions from planarity being found for the most hindered *N*-tosylated derivatives **6**. VEH calculations are used to rationalize the redox potentials and justify the low oxidation potentials measured for compounds **7** and **8**. They also show the charge-transfer nature of the lowest-energy HOMO → LUMO electronic transition, thus supporting the experimental UV-vis results. The higher oxidation potentials and blue-shifted absorption bands observed for compounds **6** are due to their highly distorted geometries which lead to a stabilization of the HOMO and a destabilization of the resulting cation-radical.

Introduction

Organic molecules containing electron donor and electron acceptor moieties constitute a very promising field of study due to the interesting optical and electronic properties they exhibit. Molecular electronics devices,[1] nonlinear optical materials (NLO),[2] and artificial photosynthetic models[3] have been proposed as potential applications for these donor–acceptor compounds.

We have recently reported the synthesis together with a detailed study of the structural, optical, and electrochemical properties of substituted benzo[*b*]naphtho[2,3-*e*][1,4]dithiin-6,11-quinones (**1a**), benzo[*b*]naphtho[2,3-*e*]oxathiin-6,11-quinones (**2a**), and their tetracyano-*p*-quinodimethane derivatives **1b** and **2b**.[4] These compounds behave as single-component donor–acceptor materials with semiconducting properties. They show a low-energy absorption band centered around 500–600 nm which was demonstrated to be due to the intramolecular electronic charge-transfer from the donor benzodithiine or benzooxathiine fragment to the acceptor benzoquinone or TCNQ rings. Compounds **1** and **2** (Figure 1) have a very rich redox chemistry giving rise to stable anions and cations.[4]

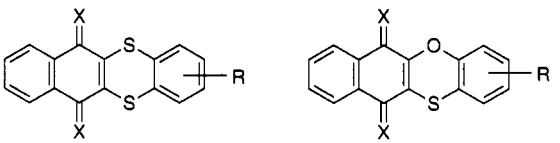

1a: X = O
1b: X = C(CN)$_2$
2a: X = O
2b: X = C(CN)$_2$

Figure 1.

In this paper we describe the synthesis of benzo[*b*]-phenoxazine-6,11-dione derivatives **7** as novel nitrogen-containing donor-acceptor systems. The *N*-tosyl substituted derivatives **6**, used synthetically as precursors for **7**, have been studied due to the striking effect the tosyl group has on the spectroscopic and electrochemical properties. The *N*-methylbenzo[*b*]phenoxazine-6,11-di-

[⊗] Abstract published in *Advance ACS Abstracts*, July 15, 1995.

(1) Metzger, R. M.; Panetta, Ch. *New J. Chem.* **1991**, *15*, 209 and references cited therein. See also: *Molecular Electronic-Science and Technology*; Aviram A., Ed.; Engineering Foundation: New York, 1989.

(2) Boyd, R. W. *Nonlinear Optics*; Academic Press: New York, 1992. Prasad, P. N.; Williams, D. J., *Introduction to Nonlinear Optical Effects in Molecules and Polymers*; Wiley: New York, 1991. Long, N. J. *Angew. Chem., Int. Ed. Engl.* **1995**, *34*, 21. Nalwa, H. S. *Adv. Mat.* **1993**, *5*, 341. Marder, S. R.; Perry, J. W. *Adv. Mat.* **1993**, *5*, 805. Brédas, J. L.; Adant, C.; Tackx, P.; Persoons, A. *Chem. Rev.* **1994**, *94*, 243. See also: Di Bella, S.; Fragalá, I. L.; Rattner, M. A.; Marks, T. J. *J. Am. Chem. Soc.* **1993**, *115*, 682. Joshi, M. V.; Cava, M. P.; Lakshmikantham, M.. V.; Metzger, R. M.; Abdeldayem, H.; Henry, M.; Venkateswarly, P. *Synth. Met.* **1993**, *57*, 3974.

(3) *Photoinduced Electron Transfer*; Fox, M. A., Chanon, M., Eds.; Elsevier: Amsterdam, 1988 and references cited therein. Danielson, E.; Elliot, C. M.; Merket, J. N.; Meyer, T. J. *J. Am. Chem. Soc.* **1987**, *109*, 2519. Wasielewski, M. R.; Niemczyk, M. P.; Svek, W. A.; Pewitt, E. B. *J. Am. Chem. Soc.* **1985**, *107*, 5562. Cowan, J. A.; Sanders, J.; Beddard, G. S.; Harrison, R. J. *J. Chem. Soc. Chem. Commun.* **1982**, 55. Gust, D.; Moore, T. A. *Science* **1989**, *244*, 35. Larson, S. L.; Cooley, L. F.; Elliot, C. M.; Kelley, D. F. *J. Am. Chem. Soc.* **1992**, *114*, 9504. Tamiaki, H.; Maruyama, K. *J. Chem. Soc. Perkin Trans. 1* **1992**, 2431.

(4) Bando, P.; Martín, N.; Segura, J. L.; Seoane, C.; Ortí, E.; Viruela, P. M.; Viruela, R.; Albert, A.; Cano, F. H. *J. Org. Chem.* **1994**, *59*, 4618.

0022-3263/95/1960-5643$09.00/0

Scheme 1

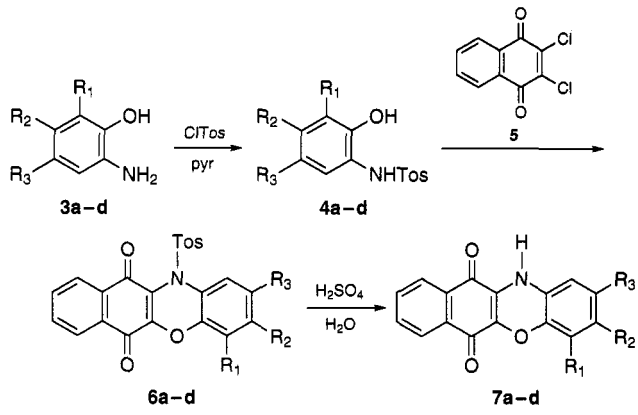

Scheme 2

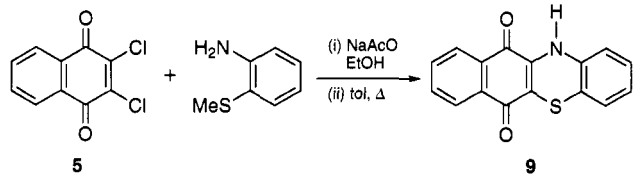

one (**8**) and the 12*H*-benzo[*b*]phenothiazine-6,11-dione (**9**) in which the oxygen atom has been replaced by a sulfur atom have also been prepared. In this study we combine cyclic voltammetry and spectroscopic UV-vis data with molecular orbital quantum-chemical calculations to characterize the compounds synthesized.

Results and Discussion

Synthesis. Compounds **6** and **7** were prepared from 2,3-dichloro-1,4-naphthoquinone (**5**) by reaction with the appropriate *N*-tosyl-2-aminophenol (**4**) in hot pyridine following the method previously reported for the unsubstituted parent compound.[5] Compounds **4** were in turn obtained from the substituted 2-aminophenols **3** by reaction with tosyl chloride as shown in Scheme 1.

Treatment of *N*-tosyl derivatives **6** under acidic conditions led to the respective 12*H*-benzo[*b*]phenoxazine-6,11-diones **7** in high yields (Scheme 1). It is worth noting that the direct reaction of the aminophenol **3** with 2,3-dichloro-1,4-naphthoquinone (**5**) led to compounds **7** in a very low yield. In the same way, the reaction of quinone **5** with 2-methylthioaniline led to the 12*H*-benzo[*b*]-phenothiazine-6,11-dione (**9**) in 15% yield (Scheme 2). Compound **9** had been prepared previously by a different method,[6] but no spectroscopic data were reported. Compound **6d** could not be characterized because of the spontaneous loss of the tosyl group during the isolation workup. Compounds **7** were obtained as stable, poorly soluble, deep blue solids in very good yields from the *N*-tosyl substituted precursors **6**. In order to increase the solubility and for comparison purposes, the more soluble *N*-methyl derivative **8** was also prepared.[7]

The compounds thus prepared are summarized in Table 1, together with some relevant spectroscopic data.

Spectroscopic Results. The electronic absorption spectra of compounds **7** show, in addition to the expected bands in the UV region, the presence of a very broad, low-energy band in the visible region centered around 650 nm (see Figure 2 and Table 1). Based on the results previously reported for compounds **1** and **2**,[4] this band is expected to arise from the intramolecular electron-transfer from the donor benzoxazine moiety to the acceptor naphthoquinone fragment of the molecule. The tosylate substituent on the nitrogen atom has a strong effect on the energy observed for this charge-transfer band. While the methyl group does not significantly alter the value of λ_{max}, the tosyl group hypsochromically shifts the band position by about 200 nm (see Figure 2 and Table 1).

Table 1. Novel Donor–Acceptor Compounds Prepared

compound	R_1	R_2	R_3	ν_{CO}[a]	λ_{max}[b] (log ϵ)
6a	H	H	H	1690	440 (2.71)
6b	H	H	Me	1690	446 (2.75)
6c	H	Me	H	1685	444 (2.92)
6d	Me	H	Me	–	–
7a	H	H	H	1660	639 (3.11)
7b	H	H	Me	1665	651 (3.02)
7c	H	Me	H	1665	652 (3.04)
7d	Me	H	Me	1670	620 (2.84)
8	H	H	H	1665	645 (3.25)
9	H	H	H	1670	698 (3.15)

[a] KBr pellets (in cm^{-1}). [b] λ_{max} (in nm) corresponds to the maximum of the lowest energy absorption band. Solvent: $CHCl_3$.

Compared with the values of λ_{max} previously observed for quinones **1a** (λ_{max} = 542 nm),[4] **2a** (λ_{max} = 548 nm),[4] and for the closely related benzo[*b*]naphtho[2,3-*e*][1,4]-dioxine-6,11-dione (λ_{max} ~ 500nm),[8] the presence of a benzoxazine unit as the donor fragment in compounds **7** and **8** drives the low energy band to significantly higher wavelength values (λ_{max} ~ 650 nm) as a consequence of the better donor character of the nitrogen atom present in **7** and **8**. This trend is also observed for the phenothiazine derivative **9** for which the measured value is even higher (λ_{max} ~ 700 nm) (see Table 1).

Electrochemical Results. The redox potentials of compounds **6-9** were measured by cyclic voltammetry at room temperature by using a glassy carbon electrode in methylene dichloride as solvent and tetrabutylammonium perchlorate as the supporting electrolyte. The voltammograms, recorded in the potential range from +2.0 to −2.0 V, evidence the presence of both reduction and oxidation waves to form stable anion and cation radicals in the same organic molecule. The redox potentials thus obtained are collected in Table 2. The cyclic voltammograms for compounds **6a** and **7a** are displayed in Figure 3.

All compounds show two one-electron reduction waves to form the corresponding anion-radical and dianion. For compounds **7–9** the two reduction waves are reversible, while for the *N*-tosyl substituted compounds **6** the first reduction potential is irreversible and the second reduction potential to the dianion is reversible (see Figure 3).

The voltammograms show the presence of a reversible oxidation wave to form the radical-cation for compounds **8** and **9** followed by a quasireversible second oxidation wave to the dication. More complex oxidation patterns are obtained for compounds **7** for which two irreversible oxidation waves are observed at *ca.* 1.0 and 1.3 V (see Figure 3 and Table 2). The presence of the tosyl substituent on the nitrogen atom in compounds **6** is responsible of the striking decrease of the oxidation

(5) Ullman, F.; Ettisch, M. *Ber. Dtsch. Chem. Ges.* **1921**, *54*, 259.
(6) Fries, K.; Kerlow, F. *Liebigs Ann. Chem.* **1922**, 218.
(7) Illescas, B.; Martín, N.; Segura, J. L.; Seoane, C.; Ortí, E.; Viruela, R.; Viruela, P. M. *J. Mat. Chem.*, in press.
(8) Gotarelli, G.; Lucarine, M.; Pedulli, G. F.; Spada, G. P. *J. Chem. Soc. Perkin Trans. 2* **1990**, 1519.

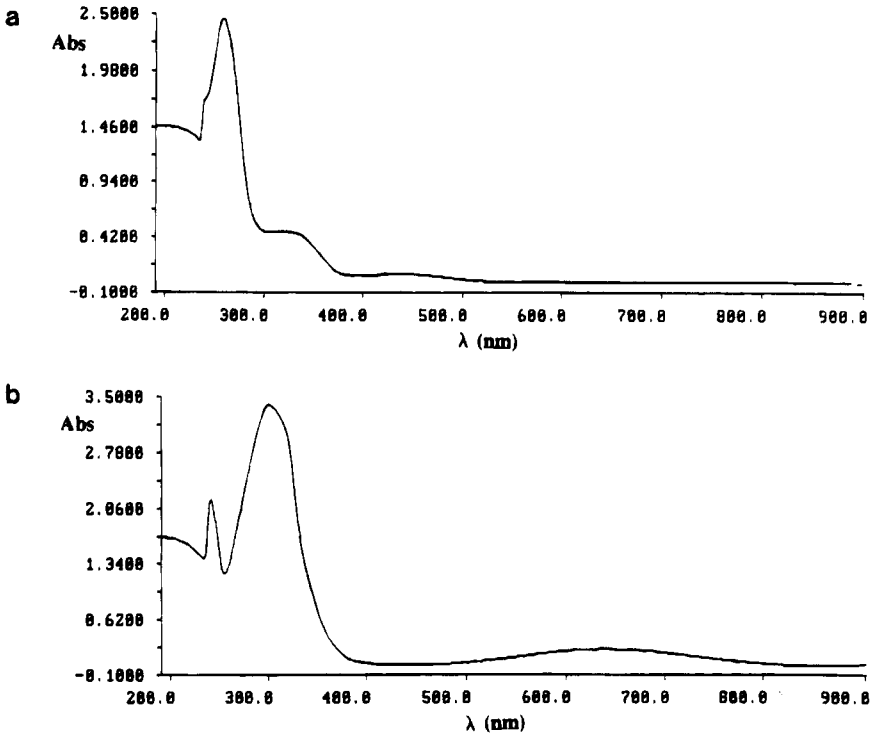

Figure 2. UV-vis spectra of compounds **6a** (a) and **7a** (b) in $CHCl_3$.

Table 2. Redox Potentials of the Donor–Acceptor Compounds (6–9) (V vs SCE)[a]

compound	$E^{1,ox}{}_{ap}$[b]	$E^{2,ox}{}_{ap}$[b]	$E^{1,red}{}_{1/2}$[c]	$E^{2,red}{}_{1/2}$[c]	ΔE	log K[d]
6a	1.75	–	−0.59	−1.13	–	–
6b	1.70	–	−0.59	−1.12	–	–
6c	1.69	–	−0.61	−1.13	–	–
7a	1.02	1.28	−0.68	−1.13	0.45	7.63
7b	1.00,[e] 1.15	1.27	−0.68	−1.13	0.45	7.63
7c	0.97,[e] 1.17	1.51	−0.69	−1.14	0.45	7.63
7d	1.10	1.49	−0.62	−1.08	0.46	7.80
8	0.98[f]	1.45[f]	−0.73	−1.19	0.46	7.80
9	0.91[f]	1.23[f]	−0.66	−1.22	0.56	9.49
TCNQ[g]	–	–	0.22	−0.36	0.58	9.76

[a] Solvent: CH_2Cl_2; scan rate: 50 mV s^{-1}. [b] Anodic peak potential. [c] Half-wave reduction potential. [d] log $K = \Delta E/0.059$; $\Delta E = E^{1,red}{}_{1/2} - E^{2,red}{}_{1/2}$. [e] Two oxidation peaks are present. [f] Reversible wave. [g] Measured in the same experimental conditions.

potential values that now appear as a single quasireversible oxidation wave at more positive voltages (see Figure 3).

The thermodynamic stability of the radical-anions has been determined from the log K values (log $K = \Delta E/0.059$).[9] Phenothiazine **9** presents a higher value of log K, thus indicating a more stable radical-anion compared with the phenoxazine derivatives **7**. The presence of the methyl group on the nitrogen atom (**8**) does not significantly alter the stability of the respective radical-anion compared with those of compounds **7**.

Theoretical Calculations. To gain some understanding of the experimental observations reported above, quantum-chemical calculations were performed at the Hartree–Fock SCF level of approximation for compounds **7a**, **8**, and **6a** as representative examples of differently *N*-substituted phenoxazindiones. The molecular geometries of these compounds were fully optimized using the MNDO-PM3 semiempirical method[10] as implemented in the MOPAC-6.0 system of programs.[11] The electronic structure was investigated by means of the nonempirical

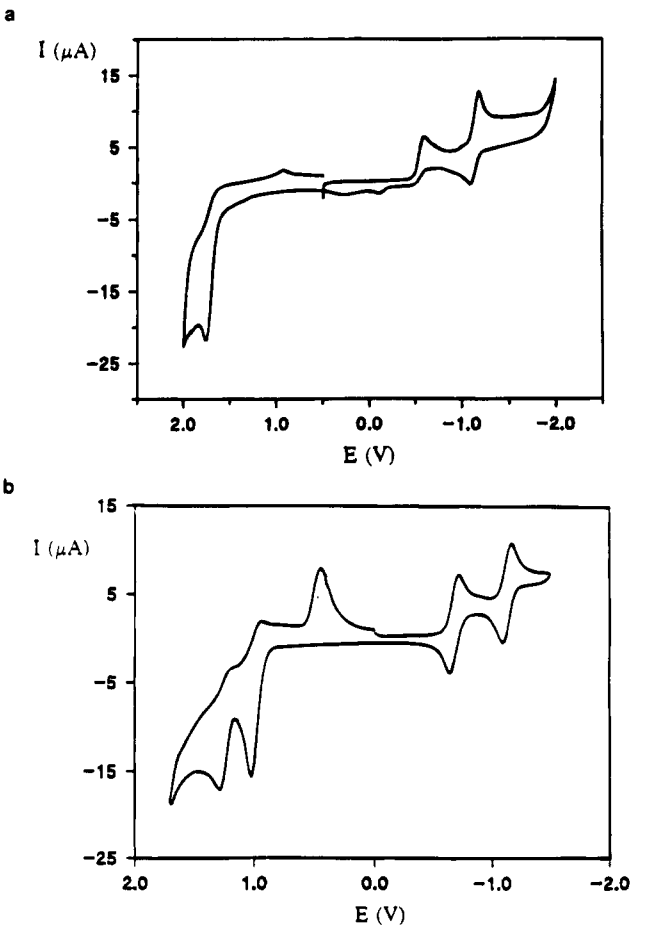

Figure 3. Cyclic voltammetries of compounds **6a** (a) and **7a** (b) in CH_2Cl_2 at room temperature (*vs* SCE).

(9) K is the coproportionation constant for the equilibrium $A + A^{2-} \rightleftharpoons 2A^{\bullet-}$ and the value of log K is calculated from the difference between the two first reduction potentials ($\Delta E = E^{1,red}{}_{1/2} - E^{2,red}{}_{1/2}$). Jensen, B. S.; Parker, V. D. *J. Am. Chem. Soc.* **1975**, *97*, 5211.

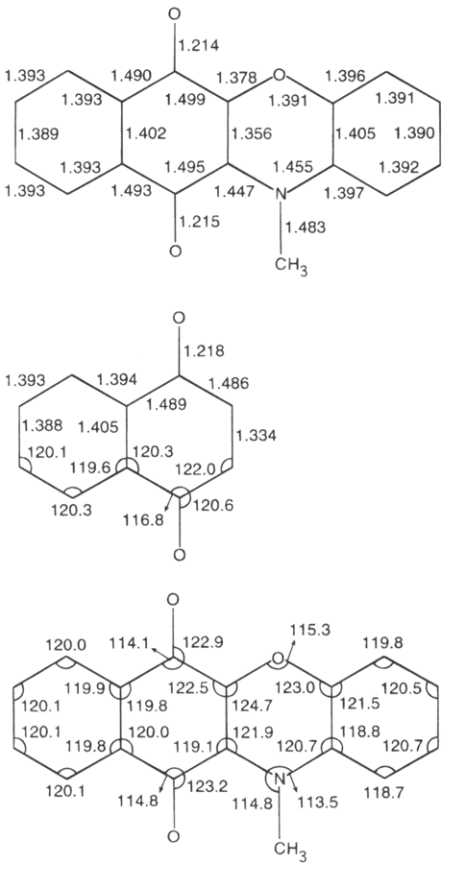

Figure 4. PM3-optimized bond lengths (top) and bond angles (bottom) calculated for **8**. The PM3 equilibrium geometry optimized for 1,4-naphthoquinone (center) is included for the sake of comparison. Bonds are in angstroms and angles in degrees.

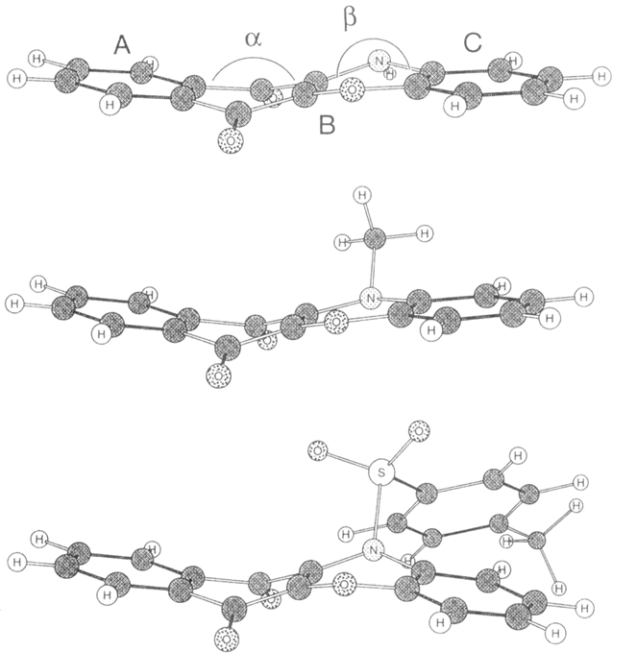

Figure 5. View showing the distortions from planarity of the PM3 equilibrium geometries calculated for **7a** (top), **8** (center), and **6a** (bottom). The most relevant molecular planes are labeled from A to C and the angles between them noted as α and β.

VEH (valence effective Hamiltonian) pseudopotential technique.[12] The VEH method takes only into account the valence electrons and is parameterized to yield one-electron energies of *ab initio* double-ζ quality. All the VEH calculations were carried out employing the atomic potentials previously optimized for hydrogen, carbon, oxygen, and nitrogen atoms.[13]

Figure 4 presents the PM3 equilibrium geometry optimized for **8** together with that obtained for 1,4-naphthoquinone. The two external benzene rings of **8** preserve their structural aromatic identity, since all the carbon−carbon bonds have a length of 1.40 ± 0.01 Å and the internal bond angles are of 120 ± 1°. The quinone ring forms a naphthoquinone moiety with the adjacent benzene ring with a geometry almost identical to that calculated for the naphthoquinone molecule. The two heteroatom bridges linking the naphthoquinone unit to the benzene ring show bond lengths significantly longer than in π-conjugated heterocycles. The nitrogen atom is joined by bonds of 1.45 Å while it has bond lengths of 1.37 Å in pyrrole.[14] This suggests that the naphthoquinone unit is poorly conjugated with the benzene ring through the heteroatom bridges. These two units are therefore expected to behave as electronically independent moieties. These trends hold also for **7a** and **6a** and for the previously reported dithiin **1a** and oxathiin **2a** naphthoquinones.[4]

The molecular structures calculated for quinones **6**−**8** are not planar (Figure 5). Theoretical calculations predict the compounds to be folded in opposite directions along the line defined by the carbonyl groups of the quinone ring and along the line passing through the heteroatom bridges. The molecule can be fitted by three planes which are labeled from A to C in Figure 5, and deviation of the molecule from planarity can be described by the angles between the planes. Angle α between planes A and B defines the bending of the naphthoquinone unit. It has a calculated value of 159.3° for **7a** and decreases to 154.0° for **8** and to 152.7° for **6a** indicating a larger deviation from planarity as the size of the substituent attached to the nitrogen bridge increases. These deviations are smaller than those predicted for **1a** (α = 142.9°) and **2a** (α = 149.3°) where the presence of sulfur bridges determines more important nonbonding interactions.[4] For 1,4-naphthoquinone, the PM3 method predicts that the conformation with α = 168.5° is slightly more stable (0.02 kcal/mol) than the fully planar conformation. Small distortions from planarity in the solid state are reported for *p*-benzoquinone[15] and 1,4-naphthoquinone.[16]

(10) Stewart, J. J. P. *J. Comput. Chem.* **1989**, *10*, 209; **1989**, *10*, 221.

(11) Stewart, J. J. P. MOPAC: A General Molecular Orbital Package (Version 6.0). *QCPE* **1990**, *10*, 455.

(12) Nicolas, G.; Durand, Ph. *J. Chem. Phys.* **1979**, *70*, 2020; **1980**, *72*, 453; André, J. M.; Burke, L. A.; Delhalle, J.; Nicolas, G.; Durand, Ph. *Int. J. Quantum Chem. Symp.* **1979**, *13*, 283. Brédas, J. L.; Chance, R. R.; Silbey, R.; Nicolas, G.; Durand, Ph. *J. Chem. Phys.* **1981**, *75*, 255.

(13) André, J. M.; Brédas, J. L.; Delhalle, J.; Vanderveken, D. J.; Vercauteren, D. P.; Fripiat, J. G., *Modern Techniques in Computational Chemistry*: MOTECC-90; Clementi, E., Ed.; Escom: Leiden, The Netherlands, 1990; p 745. Brédas, J. L.; Thémans, B.; André, J. M. *J. Chem. Phys.* **1983**, *78*, 6137.

(14) Nygaard, L.; Nielsen, J. T.; Kirchheiner, J.; Maltesen, G.; Rastrup-Andersen, J.; Sorensen, G. O. *J. Mol. Struct.* **1969**, *3*, 491.

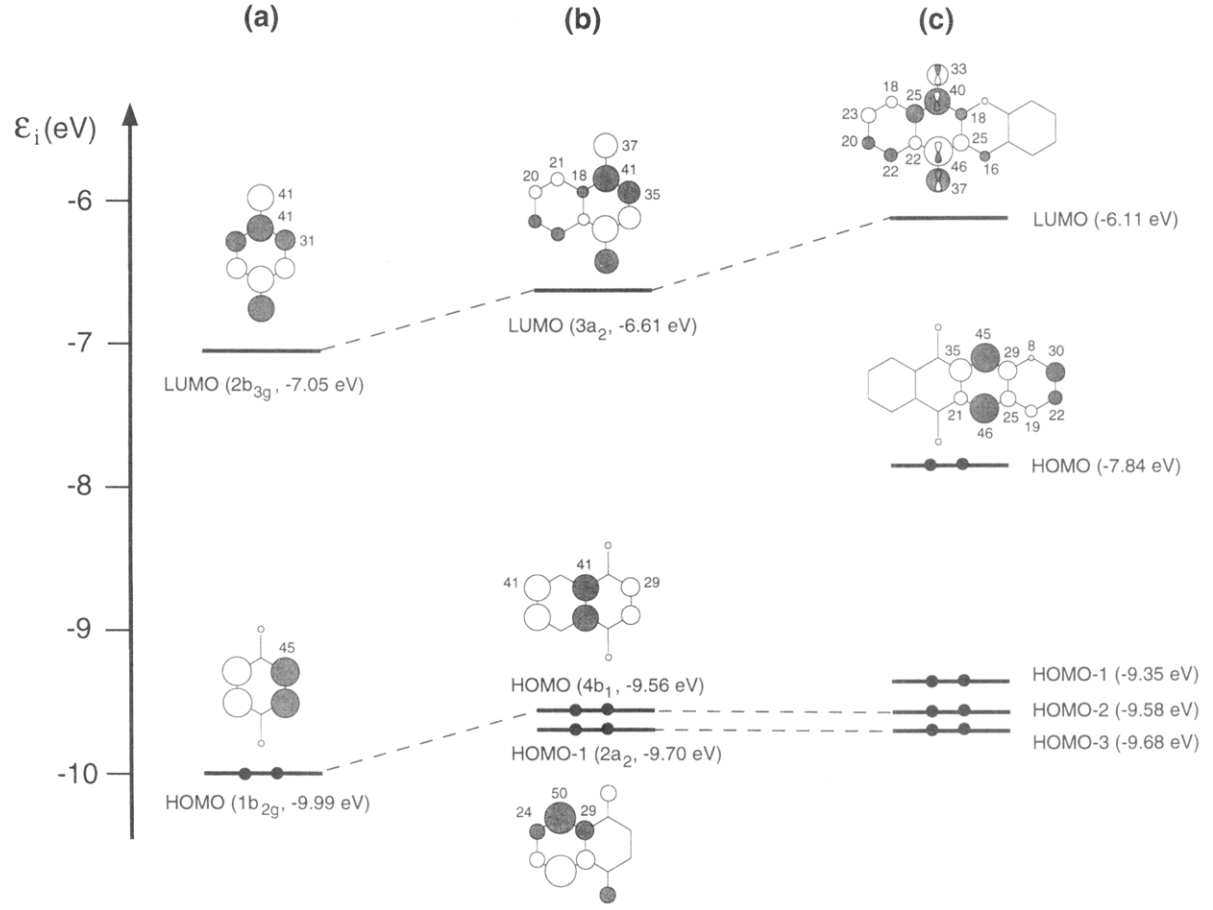

Figure 6. VEH molecular orbital diagram showing the energies, symmetries, and atomic orbital composition of the highest occupied and lowest unoccupied molecular orbitals of (a) *p*-benzoquinone (D_{2h} symmetry), (b) 1,4-naphthoquinone (C_{2v} symmetry), and quinone **7a** (no symmetry). The atomic orbital (AO) coefficients are given in units of 10^{-2}. Contributions lower than 0.15 are not displayed.

β in Figure 5 is the angle between planes B and C and measures the bending of the phenoxazine ring. This angle is predicted to be 198.2° for **7a** and 188.9° for **8**. As can be seen from Figure 5, the nitrogen atom of **8** presents a larger pyramidalization and in opposite direction than in **7a** in order to reduce the steric interactions between the methyl group and the adjacent C=O unit. For compound **6a**, the phenoxazine ring is more highly bent (β = 205.9°) due to the presence of the more voluminous tosyl group which is oriented as in **8**.

The correlation diagram sketched in Figure 6 summarizes the VEH energies, symmetries, and atomic orbital composition of the highest occupied molecular orbitals (HOMOs) and lowest unoccupied molecular orbitals (LUMOs) calculated for *p*-benzoquinone, 1,4-naphthoquinone, and **7a** using the PM3 equilibrium geometries. The LUMO shows the same atomic orbital patterns for the three compounds with strong antibonding interactions on double bonds and bonding interactions on single bonds. The fusion of a benzene ring in going from benzoquinone to naphthoquinone destabilizes this orbital by 0.44 eV due to the antibonding interactions with the quinone ring. This destabilization agrees with the more negative first reduction potential observed for naphthoquinone (−0.61 V) compared with that of benzoquinone (−0.43 V).[17] The LUMO of quinone **7a** is mainly localized on the naphthoquinone moiety and is destabilized with respect to the LUMO of naphthoquinone by the loss of planarity of the quinone ring and by the appearance of weak nonbonding interactions with the heteroatom bridges. Identical atomic orbital patterns and similar energies are found for the LUMO of **6a** and **8**. Despite the destabilization of the LUMO the first reduction potentials of **6a** (−0.59 V), **7a** (−0.68 V), and **8** (−0.73 V) are similar or slightly more negative than for naphthoquinone.

To provide a deeper insight into the effects of the reduction process the geometric structure of the anions was optimized using the PM3 method and the spin-unrestricted Hartree–Fock (UHF) formalism.[18] Figure 7a displays the most significant PM3-optimized geometric parameters of $\mathbf{8}^{\bullet-}$ as a representative example. The quinone ring is the most affected by the introduction of the extra electron. It has a more aromatic character and is completely planar like in naphthoquinone. A similar stability is therefore to be expected for the anions of **8** and naphthoquinone. Furthermore, the analysis of the net atomic charge distribution calculated for $\mathbf{8}^{\bullet-}$ reveals that the naphthoquinone moiety receives 0.82 e^- with the remaining 0.18 e^- distributed in the rest of the molecule. This result suggests that the extra electron is more

(15) van Bolhuis, F.; Kiers, C. Th. *Acta Crystallogr. B.* **1978**, *34*, 1015.
(16) Gaultier, J.; Hauw, Ch. *Acta Crystallogr.* **1965**, *18*, 179.
(17) Amlöf, J. E.; Feyereisen, M. W.; Jozefiak, T. H.; Miller, L. L. *J. Am. Chem. Soc.* **1990**, *112*, 1206.
(18) Pople, J. A.; Nesbet, R. K. *J. Chem. Phys.* **1954**, *22*, 571.

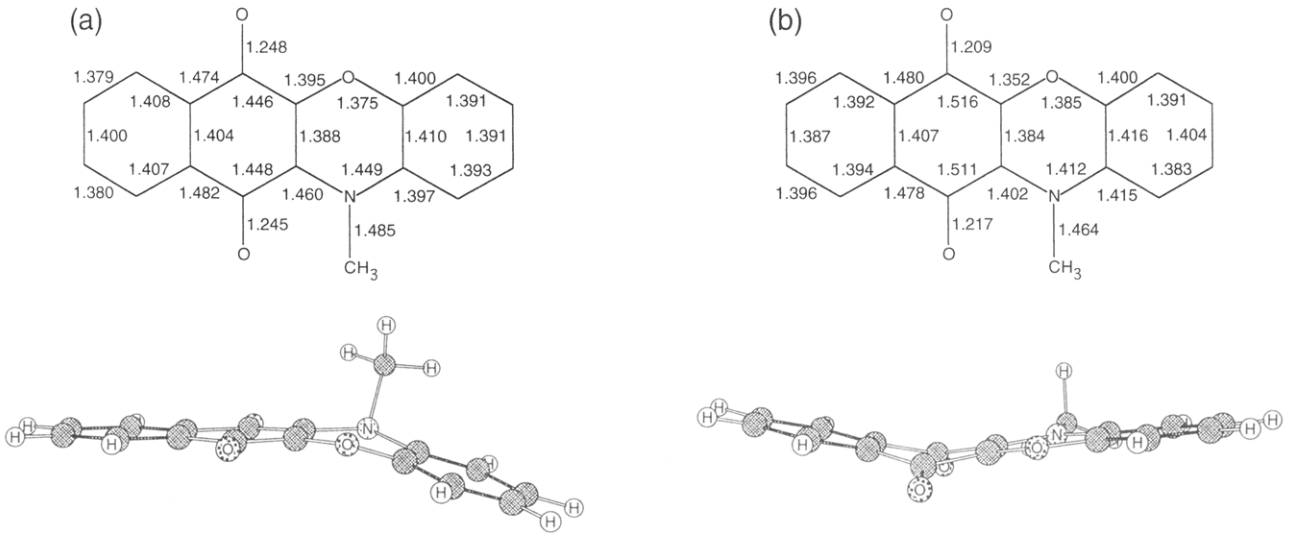

Figure 7. PM3-optimized bond lengths (Å) of the anion (a) and cation (b) of quinone **8**. No symmetry restriction was assumed during the optimization process.

delocalized for $\mathbf{8}^{\bullet-}$ than for the anion of naphthoquinone. This delocalization together with the planarity of $\mathbf{8}^{\bullet-}$ justify the fact that, although the LUMO of **8** (−6.02 eV) is significantly destabilized with respect to the LUMO of naphthoquinone (−6.61 eV), the first reduction potential of **8** (−0.73 V) is only 0.12 V more negative than that of naphthoquinone (−0.61 eV).[17] The effect of the larger delocalization of the extra charge for quinones **6**−**8** is more pronounced for the dianion. The PM3 net atomic charges calculated for $\mathbf{8}^{2-}$ show that the naphthoquinone moiety accommodates 1.64 e^- while the rest of the molecule incorporates the remaining 0.36 e^-. This result explains the considerably less negative second reduction potential obtained for quinones **6**−**8** (e.g., −1.19 V for **8**) compared with that measured for naphthoquinone (−1.41 V).[17]

We turn now to discuss the donor properties of quinones **6**−**8**. Figure 6 shows that the HOMO of naphthoquinone (−9.56 eV) has the same atomic orbital composition as the HOMO of benzoquinone (−9.99 eV). This is not the case for the HOMO of **7a** which is mainly located on the phenoxazine ring and specially on the heteroatoms. The molecular orbital correlating with the HOMO of benzoquinone and naphthoquinone corresponds to the HOMO-2 in **7a** which is actually calculated at the same energy (−9.58 eV) as in naphthoquinone. The HOMO of the quinone **7a** is therefore calculated to be ~1.7 eV higher in energy than the HOMO of naphthoquinone justifying the low oxidation potential measured for **7a** (1.02 V) which forms stable radical cations. Figure 7b displays the molecular geometry optimized for $\mathbf{8}^{\bullet+}$. The oxidation process mainly affects the phenoxazine ring since the HOMO, from which the electron is extracted, is mainly located on this part of the molecule. The phenoxazine moiety is now planar and the N−C bond lengths are reduced to 1.40−1.41 Å.

It is interesting to discuss separately the case of *N*-tosylated quinones **6**. These compounds present an oxidation potential ~0.7 V larger than N-methylated or NH quinones (see Table 2). The HOMO of **6a** shows the same atomic orbital composition than that displayed in Figure 6 for **7a** and has no contribution from the tosyl group. At the PM3 level (**6a** cannot be calculated with the VEH method since the sulfur atom environment in **6a** is not parameterized) the HOMO is calculated to be stabilized by 0.42 eV with respect to **7a**. This stabilization is due to the larger folding of the phenoxazine ring in **6a** which reduces the antibonding interactions between the heteroatom bridges and the adjacent carbon atoms. It suggests that the electron is more difficult to extract from the HOMO of **6a** in accord with the larger oxidation potential observed experimentally for compounds **6**. Furthermore, the geometry optimized for the oxidized compound reveals that, contrary to **7a** and **8**, the phenoxazine ring of $\mathbf{6a}^{\bullet+}$ is still distorted from planarity (β = 192°) and the nitrogen atom is largely pyramidalized. This is due to the large size of the tosyl group which prevents the cation to achieve planarity. The cation is therefore destabilized with respect to those formed in quinones **7** and **8**.

We finally discuss the molecular orbital interpretation of the optical absorption properties displayed by the quinones studied in this work. The 1,4-naphthoquinone molecule is taken as a reference system. The VEH molecular orbital diagram of Figure 6 shows that the HOMO ($4b_1$, −9.56 eV) and the HOMO-1 ($2a_2$, −9.70 eV) of 1,4-naphthoquinone are very close in energy. These orbitals are separated from the rest of the occupied molecular orbitals by an energy gap of 1.24 eV. Since the LUMO is also separated by more than 2 eV from the rest of unoccupied orbitals, the lowest-energy absorption band of 1,4-naphthoquinone can be attributed as resulting from the HOMO → LUMO (421 nm, long-axis polarized) and the HOMO-1 → LUMO (402 nm, short-axis polarized) electronic transitions. The electronic spectrum of unsubstituted 1,4-naphthoquinone shows an absorption band between 280 and 400 nm which is experimentally interpreted in terms of two transitions: the lowest energy one polarized along the long axis of the molecule, and the highest energy one polarized along the short axis.[19,20] Compared to experiment, the polarizations predicted by the VEH method are interchanged because this method calculates the $4b_1$ HOMO of 1,4-naphthoquinone too high in energy. This has been corroborated by an *ab initio* calculation on 1,4-naphtho-

(19) Fukuda, M.; Tajiri, A.; Oda, M.; Hatano, M. *Bull. Chem. Soc. Jpn.* **1983**, *56*, 592.
(20) Gotarelli, G.; Spada, G. P. *J. Chem. Soc. Perkin Trans. 2* **1984**, 1501.

quinone using the polarized double-ζ 6-31G** basis set[21] which predicts the $2a_2$ orbital as the HOMO and the $4b_1$ as the HOMO-1 in accord with the experimental polarizations. Compared to standard *ab initio* Hartree–Fock calculations the use of the VEH method has however the advantage of providing good estimates for the lowest-energy optical transitions.[22,23]

As discussed above, the HOMO of naphthoquinone appears at similar energies for **7a** and corresponds to the HOMO-2 while the LUMO is destabilized. These results imply that the longest-wavelength absorption band of naphthoquinone is hypsochromically shifted when passing to **7a** and no longer corresponds to the HOMO → LUMO electronic transition. This is exactly what is experimentally observed for quinones **6–8** (see Figure 2). The absorption band of naphthoquinone is now placed around 310 nm and a broad absorption band appears at higher wavelengths about 640 nm for quinones **7** and **8** and about 440 nm for **6**. This new band originates in the HOMO → LUMO transition which, as depicted in Figure 6, involves an electronic charge transfer from the phenoxazine ring, where the HOMO is located, to the naphthoquinone moiety where the LUMO is spread. The HOMO → LUMO transition is predicted to have an energy of 1.88 eV (658 nm) for **8** in excellent accord with the experimental value (645 nm). VEH calculations therefore support the intramolecular charge-transfer nature of the lowest-energy absorption band observed experimentally. The existence of this charge-transfer band has previously been predicted for other naphthoquinones with oxygen and sulfur bridges like **1a** and **2a**.[4,8] The blue shift of this band for *N*-tosylated quinones is due to the more folded structures presented by these compounds. The larger folding determines the stabilization of the HOMO and a slight destabilization of the LUMO compared with the less hindered quinones **7** and **8** and therefore opens a larger HOMO–LUMO energy gap.

Summary and Conclusions

We have carried out the synthesis of novel quinone-type donor–acceptor molecules. The synthetic strategy leads to the *N*-tosylbenzo[*b*]phenoxazine-6,11-diones **6a–d** as precursors for the 12*H*-benzo[*b*]phenoxazine-6,11-diones **7a–d**. The UV-vis spectra of these compounds (**6**, **7**) reveal the presence of a low energy charge-transfer band in the visible region, in addition to the expected UV bands. This band is bathochromically shifted depending upon the substitution on the donor fragment of the molecule. The electron donor–acceptor character of compounds **6**, **7** has been studied by cyclic voltammetry measurements. Compounds **7** show two reversible reduction waves to the radical-anion and dianion at negative potential values and also two quasireversible oxidation waves at positive values. A tosyl group on the nitrogen atom exerts an important influence on the electronic absorption spectra and the redox potentials. Thus, *N*-tosyl derivatives **6a–d** show a large hypsochromic shift of the lowest-energy absorption band and a striking decrease of the donor ability of the benzoxazine fragment.

For comparison purposes, the *N*-methylphenoxazine derivative **8** and the parent benzo[*b*]phenothiazine **9** have also been prepared. Unlike the *N*-tosyl derivatives, the photoinduced charge-transfer and the electrochemical potentials measured for the *N*-methyl compound **8** are similar to those found for the unsubstituted phenoxazine derivatives **7a–d**. However, the replacement of an oxygen atom by a sulfur in **9** leads to a significant bathochromic shift of the electron-transfer band in the visible region and to a moderate increase of the donor ability of the benzothiazine moiety which presents two reversible waves at positive values.

Semiempirical PM3 molecular orbital calculations were performed to optimize the molecular geometries of quinones **6–8**. Calculations predict that the naphthoquinone moiety retains its structural characteristics in compounds **6–8** and that the molecules are folded in opposite directions along the line defined by the carbonyl groups of the quinone ring and along the line linking the heteroatom bridges. The degree of folding depends on the substituents with the largest distortions from planarity being found for the N-tosylated derivatives **6**.

The electrochemical properties of compounds **6–8** have been rationalized on the basis of VEH calculations on the neutral compounds and PM3 optimizations of the reduced and oxidized compounds. The destabilization of the LUMO and the larger delocalization of the extra electrons are the factors invoked to explain the slightly more negative first reduction potentials and the less negative second reduction potentials measured for quinones **6–8** as compared with naphthoquinone. The low oxidation potential exhibited by quinones **7** and **8** is due to the high energy HOMO provided by the phenoxazine moiety. The more distorted structure of the N-tosylated quinones **6** stabilizes this HOMO increasing the oxidation potential.

VEH calculations predict that the HOMO → LUMO transition corresponds to an electronic transfer from the phenoxazine moiety, acting as a donor, to the acceptor naphthoquinone moiety. This result supports the intramolecular charge-transfer nature of the lowest-energy absorption band observed experimentally for quinones **6–8**. The second absorption band of these compounds corresponds to the lowest-energy absorption band of 1,4-naphthoquinone which is hypsochromically shifted due to the destabilization of the LUMO in **6–8**.

Experimental Section

***N*-Tosyl-2-aminophenols 4.** These compounds were prepared by a literature procedure.[24] ***N*-Tosyl-2-aminophenol (4a)** (95%), mp 138–139 °C. ***N*-Tosyl-4-methyl-2-aminophenol (4b)** (56%), mp 145–148 °C. ***N*-Tosyl-4,6-dimethyl-2-aminophenol (4d)** (95%), mp 123–126 °C.

***N*-Tosylphenoxazinediones 6. General Procedure.** To a solution of the corresponding *N*-tosyl-2-aminophenol (5 mmol) in pyridine (2.5 mL) at 100 °C, the 2,3-dichloro-1,4-naphthoquinone **5** (5 mmol) was added, and the mixture was stirred for 30 min. Ethanol (10–15 mL) was added, and the mixture was allowed to cool. The precipitate was filtered, washed with ethanol and hot water, and recrystallized from ethanol.

***N*-Tosylbenzo[*b*]phenoxazine-6,11-dione (6a):** 79% yield; mp 319–320 °C (lit. 320 °C);[5] ^{1}H NMR ($CDCl_3$; 300 MHz) δ 8.26 (1H, dd, J = 7.5 Hz, J = 1.8 Hz), 8.16 (1H, dd, J = 7.5 Hz, J = 1.8 Hz), 7.84 (1H, dt, J = 7.5 Hz, J = 1.8 Hz), 7.79 (1H, dt, J = 7.5 Hz, J = 1.8 Hz), 7.63–7.59 (1H, m), 7.37 (2H, d, J = 8.4 Hz), 7.27–7.20 (2H, m), 7.14 (2H, d, J = 8.4), 7.1–

(21) Hariharan, P. C.; Pople, J. A. *Theor. Chim. Acta* **1973**, *28*, 213.
(22) Brédas, J. L.; Thémans, B.; André, J. M. *J. Chem. Phys.* **1983**, *70*, 6137.
(23) Viruela-Martín, R.; Viruela-Martín, P. M.; Ortí, E. *J. Chem. Phys.* **1992**, *97*, 8470.
(24) Kurita, K. *Chem. Ind.* **1974**, 345.

6.97 (1H, m), 2.38 (3H, s); ^{13}C NMR ($CDCl_3$; 250 MHz) δ 179.4, 177.7, 151.3, 149.4, 145.6, 135.0, 134.0, 132.4, 131.6, 130.3, 129.7, 129.0, 128.4, 127.6, 126.8, 126.7, 126.2, 117.5, 117.4, 21.8; IR (KBr) 1690, 1630, 1600, 1580, 1490, 1370, 1250, 1175, 980, 770, 720, 665 cm^{-1}; MS *m/z* 263 (100), 235 (8), 179 (10), 105 (11), 104 (17), 77 (12), 76 (29); UV-vis ($CHCl_3$) λ_{max} (log ϵ) 440 (2.71), 322 (3.59), 258 (4.32), 240 (4.16). Anal. Calcd for $C_{23}H_{15}NO_5S$: C, 66.19; H, 3.60; N, 3.36. Found: C, 65.93; H, 3.62; N, 3.22.

***N*-Tosyl-2-methylbenzo[*b*]phenoxazine-6,11-dione (6b):** 63% yield; mp > 400 °C; ^{1}H NMR ($CDCl_3$; 300 MHz) δ 8.26 (1H, d, J = 7.5 Hz), 8.15 (1H, d, J = 7.5 Hz), 7.86–7.75 (2H, m), 7.43 (1H, s), 7.36 (2H, d, J = 8.1 Hz), 7.14 (2H, d, J = 8.1 Hz), 7.02 (1H, d, J = 8.4 Hz), 6.86 (1H, d, J = 8.4 Hz), 2.38 (3H, s), 2.37 (3H, s); ^{13}C NMR (DMSO; 250 MHz) δ 183.8, 171.9, 164.9, 147.6, 144.6, 134.4, 133.5, 131.6, 131.1, 129.7, 128.1, 126.9, 126.0, 125.7, 124.9, 112.1, 21.0, 20.4; IR (KBr) 1690, 1630, 1600, 1575, 1500, 1370, 1270, 1210, 1175, 990, 720, 670 cm^{-1}; MS *m/z* 277 (76), 251 (41), 223 (100), 222 (14), 179 (94), 166 (18), 139 (20), 104 (56), 88 (24), 83 (30), 76 (61), 62 (24), 51 (25); UV-vis ($CHCl_3$) λ_{max} (log ϵ) 446 (2.75), 329 (3.67), 263 (4.31), 239 (4.21). Anal. Calcd for $C_{24}H_{17}NO_5S$: C, 66.82; H, 3.94; N, 3.25. Found: C, 66.59; H, 3.93; N, 3.26.

***N*-Tosyl-3-methylbenzo[*b*]phenoxazine-6,11-dione (6c):** 90% yield; mp 167–169 °C; ^{1}H NMR ($CDCl_3$; 300 MHz) δ 8.25 (1H, d, J = 7.5 Hz), 8.14 (1H, d, J = 7.5 Hz), 7.86–7.75 (2H, m), 7.45 (1H, d, J = 8.4 Hz), 7.35 (2H, d, J = 8.1 Hz), 7.15 (2H, d, J = 8.1 Hz), 7.02 (1H, d, J = 8.4 Hz), 6.80 (1H, s), 2.39 (3H, s), 2.32 (3H, s); ^{13}C NMR (DMSO; 250 MHz) δ 183.8, 171.9, 164.9, 147.6, 144.6, 134.4, 133.5, 131.6, 131.1, 129.7, 128.1, 126.9, 126.0, 125.7, 124.9, 112.1, 21.0, 20.4; IR (KBr) 1685, 1630, 1600, 1580, 1500, 1375, 1265, 1175, 990, 850, 720, 665 cm^{-1}; MS *m/z* 277 (100), 248 (10), 104 (14), 89 (11), 76 (15), 51 (9); UV-vis ($CHCl_3$) λ_{max} (log ϵ) 444 (2.92), 320 (3.63), 263 (4.27), 240 (4.17). Anal. Calcd for $C_{24}H_{17}NO_5S$: C, 66.82; H, 3.94; N, 3.25. Found: C, 66.73; H, 3.88; N, 3.27.

12*H*-Phenoxazinediones 7. General Procedure. Sulfuric acid (3.5 mL) was added with stirring to the *N*-tosylphenoxazindiones (1 mmol) in a well closed flask. After 30 min, the reaction mixture was cooled at 0 °C and water (35 mL) was added dropwise with vigorous stirring. The precipitate was filtered and washed with hot water. It was crystallized from acetonitrile.

12*H*-Benzo[*b*]phenoxazine-6,11-dione (7a): 95% yield; mp 293–294 °C; ^{1}H NMR (DMSO; 300 MHz) δ 8.86 (1H, s), 7.94 (2H, dd, J = 7.2 Hz, J = 1.5 Hz), 7.84 (1H, dt, J = 7.2 Hz, J = 1.5 Hz), 7.77 (1H, dt, J = 7.2 Hz, J = 1.5 Hz), 6.82–6.67 (4H, m); IR (KBr) 3350, 1640, 1600, 1580, 1515, 1500, 1450, 1370, 1340, 1270, 1180, 980, 755, 715 cm^{-1}; MS *m/z* 263 (M^+, 100), 235 (11), 179 (14), 152 (11), 104 (20), 76 (32); UV-vis ($CHCl_3$) λ_{max} (log ϵ) 639 (3.11), 382 (4.25), 241 (4.06). Anal. Calcd for $C_{16}H_9NO_3C$: C, 73.00; H, 3.42; N, 5.32. Found: C, 72.89; H, 3.59; N, 5.46.

12*H*-2-Methylbenzo[*b*]phenoxazine-6,11-dione (7b): 90% yield; mp 252–253 °C; ^{1}H NMR (DMSO; 300 MHz) δ 8.80 (1H, s), 7.90 (2H, d, J = 7.2 Hz), 7.82–7.70 (3H, m), 6.92 (1H, s), 6.55 (1H, s), 2.20 (3H, s); IR (KBr) 3310, 1665, 1625, 1590, 1570, 1470, 1390, 1355, 1305, 1180, 970, 890, 710, 680 cm^{-1}; MS *m/z* 277 (M^+, 90), 248 (10), 104 (20), 89 (13), 79 (100), 76 (19), 63 (13), 52 (89), 51 (45); UV-vis ($CHCl_3$) λ_{max} (log λ) 651 (3.02), 306 (4.06), 241 (3.95). Anal. Calcd for $C_{17}H_{11}NO_3$: C, 73.65; H, 3.97; N, 5.05. Found: C, 73.67; H, 3.95; N, 4.98.

12*H*-3-Methylbenzo[*b*]phenoxazine-6,11-dione (7c): 90% yield; mp 281 °C dec; ^{1}H NMR (DMSO; 300 MHz) δ 8.81 (1H, s), 7.90 (2H, dd, J = 7.5 Hz, J = 1.5 Hz), 7.80 (1H, dt, J = 7.5 Hz, J = 1.5 Hz), 7.72 (1H, dt, J = 7.5 Hz, J = 1.5 Hz), 6.67 (1H, d, J = 7.8 Hz), 6.56 (1H, d, J = 7.8 Hz), 6.5 (1H, s), 2.09 (3H, s); IR (KBr) 3320, 1665, 1650, 1620, 1600, 1580, 1520, 1495, 1475, 1365, 1340, 1270, 1190, 820, 720 cm^{-1}; MS *m/z* 277 (M^+, 100), 248 (10), 220 (5), 165 (6), 139 (6), 104 (14), 89 (10), 76 (13), 51 (7); UV-vis ($CHCl_3$) λ_{max} (log ϵ) 652 (3.04), 307 (4.23), 242 (4.10). Anal. Calcd for $C_{17}H_{11}NO_3$: C, 73.65; H, 3.97; N, 5.05. Found: C, 73.35; H, 3.84; N, 4.95.

12*H*-2,4-Dimethylbenzo[*b*]phenoxazine-6,11-dione (7d): 85% yield; mp 263–264 °C; IR (KBr) 3360, 1670, 1640, 1605, 1485, 1360, 1310, 1150, 990, 730, 700 cm^{-1}; UV-vis ($CHCl_3$) λ_{max} (log ϵ) 620 (2.84), 310 (4.19), 243 (4.20). Anal. Calcd for $C_{18}H_{13}NO_3$: C, 74.08; H, 4.47; N, 4.81. Found: C, 73.77; H, 4.42; N, 4.53.

12*H*-Benzo[*b*]phenothiazine-6,11-dione (9). To a suspension of 2,3-dichloro-1,4-naphthoquinone (**5**) (0.025 mol) and sodium acetate (0.061 mol) in dried ethanol (50 mL), 2-(methylthio)aniline (0.025 mol) was added with stirring under argon atmosphere. The mixture was refluxed for 5 h. The solvent was evaporated, and toluene (50 mL) was added and the mixture refluxed at 140 °C for 24 h. The reaction mixture was allowed to cool and the precipitate was filtered and washed with ethanol and hot water. It was crystallized from chlorobenzene: 15% yield; mp 306–308 °C (lit. 308 °C);[6] ^{1}H NMR (DMSO; 300 MHz) δ 9.01 (1H, s), 7.96 (1H, dd, J = 7.8 Hz, J = 1.5 Hz), 7.88 (1H, dd, J = 7.8 Hz, J = 1.5 Hz), 7.81 (1H, dt, J = 7.8 Hz, J = 1.5 Hz), 7.75 (1H, dt, J = 7.8 Hz, J = 1.5 Hz), 7.01 (1H, d, J = 8.1 Hz), 6.93–6.87 (1H, m), 6.79–6.77 (2H, m); IR (KBr) 3240, 1670, 1610, 1595, 1570, 1565, 1475, 1435, 1355, 1290, 1245, 1150, 850, 750, 720 cm^{-1}; MS *m/z* 281 (19), 279 (M^+, 100), 222 (18), 139 (12), 121 (20), 111 (15), 104 (15), 98 (11), 89 (17), 76 (25); UV-vis ($CHCl_3$) λ_{max} (log ϵ) 698 (3.15), 316 (4.02), 244 (4.02). Anal. Calcd for $C_{16}H_9NO_2S$: C, 68.80; H, 3.23; N, 5.01. Found: C, 68.76; H, 3.38; N, 4.90.

Acknowledgment. This work has been supported by the DGICYT Projects PB92-0237 and PB91-0935 and the European Commission (Contract ERB. CI1*-CT 93-0066). The authors thank the CIUV (Centro de Informática de la Universitat de València) for the use of their computing facilities.

JO950368S